

Characterization of electrodeposited nickel film surfaces using atomic force microscopy

M. Saitou, W. Oshikawa and A. Makabe

Dept. of Mechanical Systems Engineering, University of the Ryukyus, 1 Senbaru
Nishihara-cho, Okinawa, 903-0213 Japan

Microstructures of nickel surfaces electrodeposited on ITO glasses are investigated using atomic force microscopy. The fractal dimension D and Hurst exponent H of the nickel surface images are determined from a frequency analysis method proposed by A. Aguilar et al., and from Hurst rescaled range analysis. The two methods are found to give the same value of the fractal dimension $D \sim 2.0$. The roughness exponent α and growth exponent β that characterize scaling behaviors of the surface growth in electrodeposition are calculated using the height-difference correlation function and interface width in Fourier space. The values of $\alpha \sim 1.0$ and $\beta \sim 0.8$ show that the surface growth does not belong to the universality classes theoretically predicted by statistical growth models.

Keywords: A. Atomic force microscopy, E. Electrochemistry, F. Fourier transform method, F. Fractal dimension, N. Nickel, S. Scaling, S. Surface roughness

1. Introduction

There have been recently considerable efforts in understanding the phenomenon of surface roughening in film growth [1]. Generally it is recognized that the surface morphology and dynamics of growing surfaces by deposition obey simple scaling laws associated with scaling exponents such as a roughness exponent α [2,3]. The roughness exponent α is determined from the height-difference correlation function $G(\mathbf{r},t)$ that has the form [4],

$$G(\mathbf{r},t) = \left\langle [h(\mathbf{r} + \mathbf{r}_1, t) - h(\mathbf{r}_1, t)]^2 \right\rangle_{\mathbf{r}_1} \propto r^{2\alpha}, \text{ for } r \ll \xi \quad (1)$$

where $h(\mathbf{r},t)$ is the surface height, $\langle \dots \rangle$ is the spatial average over the measured area, and ξ the correlation length. The quantity of α characterizes the roughness of the surfaces and can be definitely related to statistical models of continuum equations that have been introduced to understand surface growth by deposition. For example, the KPZ equation [5] is represented by

$$\partial h(r,t) / \partial t = \nu \nabla^2 h(r,t) + \lambda (\nabla h(r,t))^2 / 2 + \eta, \quad (2)$$

where ν is the surface tension, λ the coefficient of the lowest order nonlinear term, and η reflects the random fluctuations in the deposition process. For the one-dimensional KPZ equation, $\alpha=1/2$ is theoretically obtained.

Many experiments [6-10] of fractal electrodeposits have revealed morphological diagrams for fractal pattern formation and the fractal structures of the electrodeposits that are similar to the computer simulation of the DLA (diffusion-limited aggregates) model generated by Witten and Sander [11]. The changes of fractal dimensions in time correspond to those of the morphology of surfaces.

Thus the growth exponent α and fractal dimension D are good indices for representing the microstructures of surfaces. In this study, nickel films were electrodeposited on ITO (indium tin oxides coated) glasses for 80-800sec at a low current density in a still nickel sulfamate bath. Atomic force microscopy (AFM) was employed to characterize the surface morphology of the electrodeposited nickel films. Russ [12] stated that methods for measuring the fractal dimension from surface images should be chosen in view of some restrictions on their use and noise effect. In particular, Aguilar and co-workers [13-16] have extensively investigated Fourier transform

methods for the fractal dimension proposed by many researchers and concluded that all measurements of the fractal dimension are doubtful. Instead of the erroneous methods they proposed a Fourier transform method called the fractal analysis by circular average (FACA), which gives a reliable fractal dimension. In this study, the FACA and the Hurst rescaled range(R/S) analysis [14] were applied to determine the fractal dimension and Hurst exponent of the nickel deposits. The Hurst rescaled range(R/S) analysis directly relates the Hurst exponent H to the fractal dimension D and can bypass noise included in the AFM images [17].

This paper investigates the fractal dimension of the AFM images of the nickel films electrodeposited on ITO glasses for 80-800sec using the FACA and R/S analysis. In our experiments, the two methods yield the same value of the fractal dimension for the surface images of the electrodeposited nickel surface. Moreover the roughness exponent α and the growth exponent β are determined from the height-difference correlation function and interface width in Fourier space.

2. Experiment and Analytical Methods

(a) Experimental procedure

ITO (indium tin oxide coated) glasses (sheet resistivity $6\Omega/$) with the rms roughness of 1.2nm cleaned by a wet process were prepared for substrates. The two ITO glass plates for cathode and anode electrodes were located parallel in a still bath containing (g/l): nickel sulfamate, 600; nickel chloride, 5; and boric acid, 40. The bath was maintained at pH 4, the temperature of 323 K and a fixed current density of 2mA/cm². The samples were scanned in air with atomic force microscopy with a resolution of 512x512 pixels. The AFM images with different scan regions of 1000x1000 and 2000x2000nm² were used for calculation of the scaling exponents.

(b) FACA [14, 16] using a Fast Fourier Transform

AFM generally gives digitized profile heights $h(k,l)$ for an image size LxL nm² comprising MxM pixels where k and l are integers in the x and y directions. The discrete Fourier transform [18] of $h(k,l)$ is

$$H(m,n) = (1/M^2) \sum_{k,l} h(k,l) \exp[-2\pi(mk + nl)/M], \quad (3)$$

where m and n are integers within [0,M-1] and the ranges of k and l are $-M/2 \leq k, l \leq M/2 - 1$. The power spectrum dependent on the frequency f yields

$$|H(m,n)|^2 \propto f^{-\gamma}. \quad (4)$$

The FACA needs to average over all directions in k space, i.e., calculate the mean value of the power spectrum on a circle in k space. The slope γ obtained from a log-log plot of Eq.(4) gives the fractal dimension expressed by

$$D = \frac{8-\gamma}{2}. \quad (5)$$

The interface width $w(L,t)$ is defined by the rms fluctuation in the surface height [2], which is related to the growth exponent β ,

$$w(L,t) = \left\langle [h(r,t) - \langle h \rangle]^2 \right\rangle^{1/2} \propto t^\beta, \quad (6)$$

where L is the system size and $\langle \dots \rangle$ is the spatial average over the measured area. Let us consider the Fourier transform of $h(r,t) - \langle h \rangle$, i.e., $h(f,t) = F\{h(r,t) - \langle h \rangle\}$. We can rewrite Eq.(6) using the Parseval property of the Fourier transform [16],

$$w(L,t) = \left\langle \frac{h(f,t)^2}{2\pi} \right\rangle^{1/2} \propto t^\beta. \quad (7)$$

In this study, using Eq.(7) defined in k space, the growth exponent β is obtained from the slope in a log-log plot of w vs t .

(c) R/S analysis [17]

Applying the R/S analysis to the AFM images, we can determine the fractal dimension. The formula for H is as follows:

$$R(k,t) / S(k,t) \propto r_k^H, \quad (8)$$

where r_k is an arbitrary radius on the AFM images,

$$R(k,t) = \max_{0 \leq i \leq k} X(i,t) - \min_{0 \leq i \leq k} X(i,t), S(k,t) = \left\{ k^{-1} \sum_{i=1}^k [h(r_i,t) - \langle h(r,t) \rangle_i]^2 \right\}^{1/2}, \quad (9)$$

and

$$X(k,t) = \sum_{i=1}^k [h(r_i,t) - \langle h(r,t) \rangle_k]. \quad (10)$$

The slope in a log-log plot of R/S vs r_k gives the fractal dimension from the relation $D = 3 - H$.

3. Results and Discussion

In order to characterize the microstructures of the nickel surfaces we evaluate the fractal dimension D , Hurst exponent H , and roughness exponent α and growth exponent β from the AFM images. The Hurst exponent [17], which varies between 0 and 1, describes the fractal characteristics of time series and $H > 0.5$ characterizes the persistence of the time series (called the memory effect). If the system ($H > 0.5$) increases in a period, it is more likely to keep increasing in the immediately next period. $H = 0.5$ means that the system obeys a random walk. Hence the Hurst exponent for electrodeposited nickel surfaces gives information on a tendency in surface growth during electrodeposition.

Fig.1 shows the AFM images of the nickel surfaces with a region of $2000 \times 2000 \text{nm}^2$ electrodeposited at the fixed current density of 2mA/cm^2 for 200, 500 and 740sec. The vertical scale of each image with a resolution of 512×512 pixels was magnified by a factor of 3.3 in order to enhance viewing. Nickel morphology appears to be continuous mounds that become larger as the process proceeds.

Fig.2 shows a typical log-log plot of $|H(m,n)|^2$ vs the frequency f calculated from the nickel film image of $2000 \times 2000 \text{nm}^2$ for 740sec. It can be seen that $|H(m,n)|^2$ decreases linearly with the frequency f and the slope γ best fitted to the data yields the fractal dimension by the FACA. As shown in Fig.3, the average value of D is 2.02 ± 0.05 that are independent of the growth time.

Fig.4 shows a log-log plot of R/S vs r_k for the AFM image of $1000 \times 1000 \text{nm}^2$ for 740sec. We obtain the Hurst exponent as follows: First, we calculate $X(k,t)$ within a radius r_k on the AFM image. Next, we find the maximum and minimum change of $X(k,t)$ and normalize $R(k,t)$ by the standard deviation $S(k,t)$. The slope yields the Hurst exponent in Eq.(8). As shown in Fig.5, the average fractal dimension D and Hurst exponent H for the nickel films grown for 80-800sec are $D = 2.04 \pm 0.02$ and $H = 0.96 \pm 0.02$.

Thus, the FACA and R/S analysis are found to give the same value of the fractal dimension. Hence the fractal dimension $D \sim 2.0$ obtained in this experiment is a reliable value. There have been several experiments [8,10] on the fractal dimension D of thin films electrodeposited on two-dimensional substrates. In spite of their surface morphology that seems to be a set of continuous mounds, the values of the fractal dimension, nearly equal to 2.5 in the DLA model, have been reported. We guess these values of the fractal dimension are doubtful because of their inappropriate methods for analysis of the fractal dimension.

Fig.6 shows a log-log plot of $G(r,t)$ vs the lateral distance r for the electrodeposited nickel films. It can be seen that $G(r,t)$ increases linearly with r and reaches a saturated value. The plateau point in Fig.6 corresponds to the correlation length ξ , which is equal to an average mound size formed on the surface. As shown in Fig.7, we obtain an average value of $\alpha = 0.96 \pm 0.04$ that is equal to the Hurst exponent determined from the R/S analysis.

Fig.8 shows $w(t)$ vs the growth time t in a log-log scale, which gives the growth exponent $\beta = 0.80 \pm 0.07$ according to Eq.(7). The values of $w(t)$ are calculated in k space. In general the theoretical value of β is $1/2$ and under [2]. The experimental value of $\beta > 1/2$ [19-21] has been tentatively explained by the Schwoebel effect [22] and shadowing [2]. Anyway the values of $\alpha \sim 1.0$ and $\beta \sim 0.8$ do not belong to any universal classes theoretically predicted by the statistical growth models.

In addition, the value of H , 0.96 indicates that there exists the memory effect during electrodeposition. As shown in Fig.1, the growth process follows a scenario that the lateral and vertical size of mounds formed on the ITO glasses increase with time and larger mounds cover smaller ones (coarsening). Hence the value of $H = 0.96$ means that the mounds will continue to grow and coarsen.

4. Conclusion

The microstructures of the electrodeposited nickel surfaces are characterized by the fractal dimension D , the Hurst exponent, the roughness exponent α , and the growth exponent β using the AFM images. The fractal dimension and Hurst exponent are determined from the FACA and R/S analysis. The two methods give the same value of the fractal dimension $D \sim 2.0$, which is a reliable value. The values of $\alpha \sim 1.0$ and $\beta \sim 0.8$ for the electrodeposited nickel films indicate that the surface growth does not belong to any universal classes theoretically predicted by the statistical growth models.

Acknowledgement

This work was supported by Grant-in-Aid for Scientific Research (C), No.13650029 by the Ministry of Education, Science, and Culture of Japan.

References

1. P. Meakin, *Fractals, scaling and growth far from equilibrium*, Cambridge Uni. Pr., 1998.
2. A. -L. Barabási and H. E. Stanley, *Fractal Concepts in Surface Growth*, Cambridge Uni. Pr., 1995.
3. B. B. Mandelbrot, *The Fractal Geometry of Nature*, Freeman, San Francisco, 1982.
4. J. H. Jeffries, J. -K. Zuo, and M. M. Craig, *Phys. Rev. Lett.*,76(1996)4931.
5. M. Kardar, G. Parisi and Y. -C. Zhang, *Phys. Rev. Lett.*, 56 (1986)889.
6. D. Grier, E. B-Jacob, R. Clarke, and L. M. Sander, *Phys. Rev. Lett.*,56 (1986)1264.
7. A. Kuhn,F. Argoul,J. F. Muzy, and A. Arneodo, *Phys. Rev. Lett.*,73(1994)2998.
8. J. M. G-Rodríguez, A. M. Baró, L. Vázquez, R. C. Salvarezza, J. M. Vara, and A.J.Arvia, *J. Phy. Chem.*, 96(1992)347.
9. S. M. Jordan, R. Scad, D. J. L. Hermann, J. F. Lawler, and H.van Kempen, *Phys. Rev. B* 58(1998)13132.
10. P. L. Antonucci, R. Barberi, A. S. Arico, A. Amoddeo, and V. Antonucci, *Mater.Sci.Eng.* B38(1996)9.
11. T. A. Witten and L. M. Sander, *Phys. Rev. Lett.*,47(1981)1400.
12. J. C. Russ, *Fractal Surface*, Plenum Press, New York,1994.
13. E. Anguiano, M. Pancorbo, and M. Aguilar, *J. Microsc.*,172(1993)223
14. M. Aguilar, E. Anguiano, and M. Pancorbo, *J. Microsc.*,172(1993)233.
15. M. Pancorbo, M. Anguiano, and M. Aguilar, *J. Microsc.*,176(1994)54.
16. A. I. Oliva, E .Anguiano, J. L. Sacedó, M. Aguilar, J. A. Méndez, and J. A. Aznárez, *Phys. Rev. B*,60(1999)2720.
- 17.J. Feder, *Fractals*, Plenum Press,1988.
- 18.Ph. Dumas, B. Bouffakhreddine, C.Amra, O. Vatel, E. Andre, R. Galindo, and F.Salvan, *Europhys.*, 22(1993)717.
- 19.S. Mendez, G. Andreasen, P. Schilardi, M. Figueroa, L. Vázquez, R. C. Salvarezza, and A. J. Arvia, *Langmuir*,14,(1998)2515.
20. H. -J. Ernst, F. Fabre, R. Folkerts, and J. Lapujoulade, *Phys. Rev. Lett.*, 72(1994)112.
21. L. Vázquez, J. M. Albella, R. C. Salvarezza, A. J. Arvia and R. A. Levy and D. Perese, *Appl. Phys. Lett.*,68(1996)1285.
22. R. L. Schwoebel and E. J. Shipsey, *J. Appl. Phys.*,37(1966)3682.

Figure Captions

Fig.1 AFM images of the nickel films grown at a fixed current density of $2\text{mA}/\text{cm}^2$ for (a)200, (b) 500, and (c) 740. Each image size is $2000 \times 2000 \text{nm}^2$ and the vertical scale of each image with a resolution of 512×512 pixels was magnified by a factor of 3.3 in order to enhance viewing.

Fig.2 Log-log plot of $|H(k_m, k_n)|^2$ vs the frequency f calculated from the AFM images of $2000 \times 2000 \text{nm}^2$ electrodeposited for 740sec. The solid line indicates a straight line with the slope γ of 4.0 best fitted to the data.

Fig.3 The plot of the fractal dimension D vs electrodeposition time t determined by the FACA. The horizontal line indicates an average value of D , 2.02 ± 0.05 .

Fig.4 Log-log plot of R/S vs r_k calculated from the AFM images of $1000 \times 1000 \text{nm}^2$ electrodeposited for 740sec. The solid line indicates a straight line with the slope H of 1.0 best fitted to the data.

Fig.5 Plot of the fractal dimension D vs electrodeposition time t determined by the R/S analysis. The horizontal line indicates an average value of D , 2.04 ± 0.02 .

Fig.6 Log-log plot of the height-difference correlation functions $G(r,t)$ vs r , calculated from the AFM images of the electrodeposited nickel films.

Fig.7 Plot of the roughness exponent α vs electrodeposition time t determined from the slopes in Fig.6. The horizontal line indicates an average value of α , 0.96 ± 0.04 .

Fig.8 Log-log plot of the interface width $w(t)$ vs electrodeposition time t , calculated from Eq.(7). The solid line indicates a straight line with the slope β of 0.80 ± 0.07 best fitted to the data.

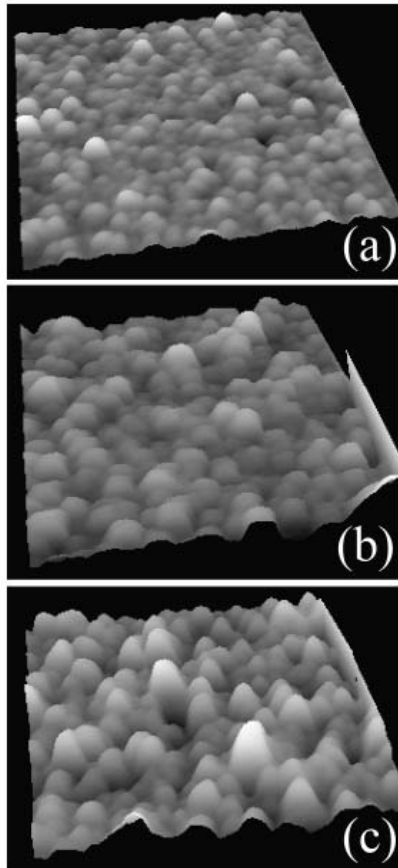


Fig.1 AFM images of the nickel films grown at a fixed current density of $2\text{mA}/\text{cm}^2$ for (a)200, (b) 500, and (c) 740. Each image size is $2000\times 2000\text{nm}^2$ and the vertical scale of each image with a resolution of 512×512 pixels was magnified by a factor of 3.3 in order to enhance viewing.

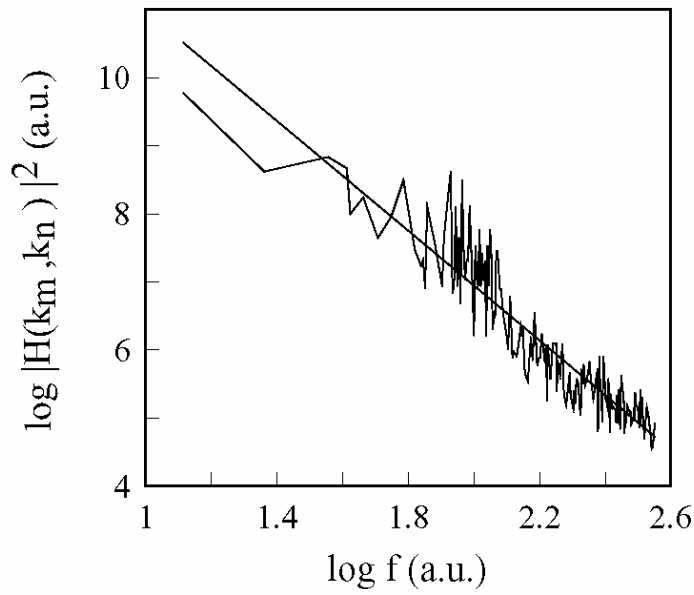


Fig.2 Log-log plot of $|H(k_m, k_n)|^2$ vs the frequency f calculated from the AFM images of $2000 \times 2000 \text{ nm}^2$ electrodeposited for 740sec. The solid line indicates a straight line with the slope γ of 4.0 best fitted to the data.

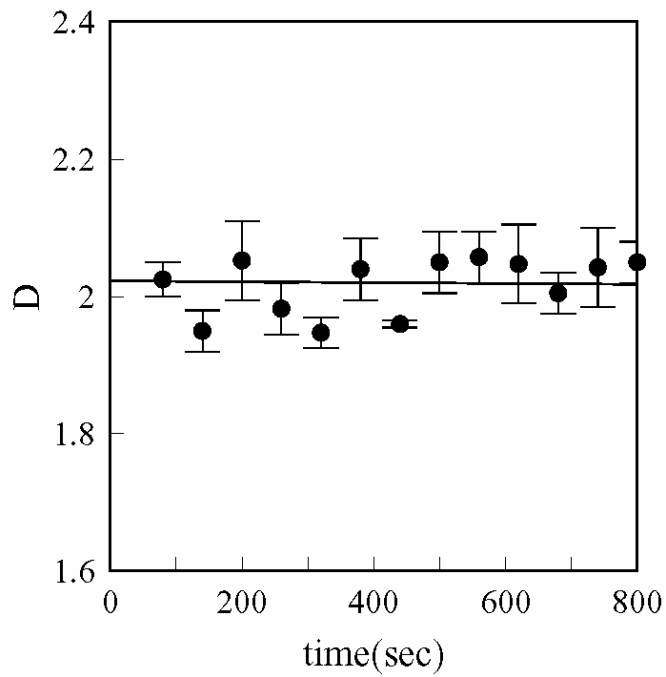


Fig.3 The plot of the fractal dimension D vs electrodeposition time t determined by the FACA. The horizontal line indicates an average value of D , 2.02 ± 0.05 .

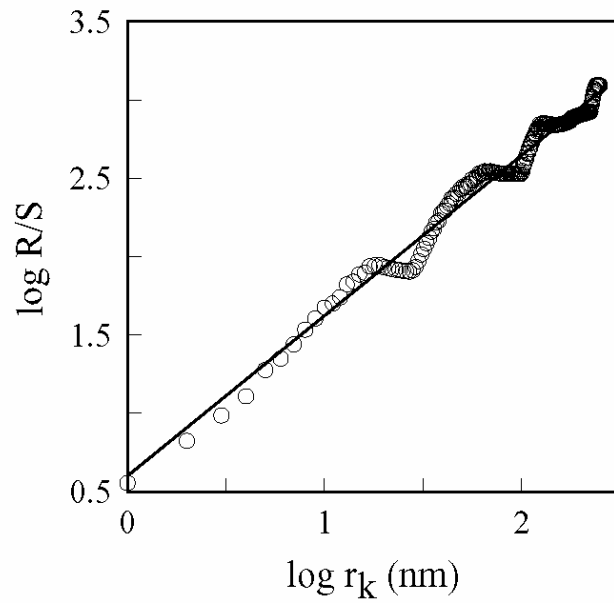


Fig.4 Log-log plot of R/S vs r_k calculated from the AFM images of $1000 \times 1000 \text{ nm}^2$ electrodeposited for 740sec. The solid line indicates a straight line with the slope H of 1.0 best fitted to the data.

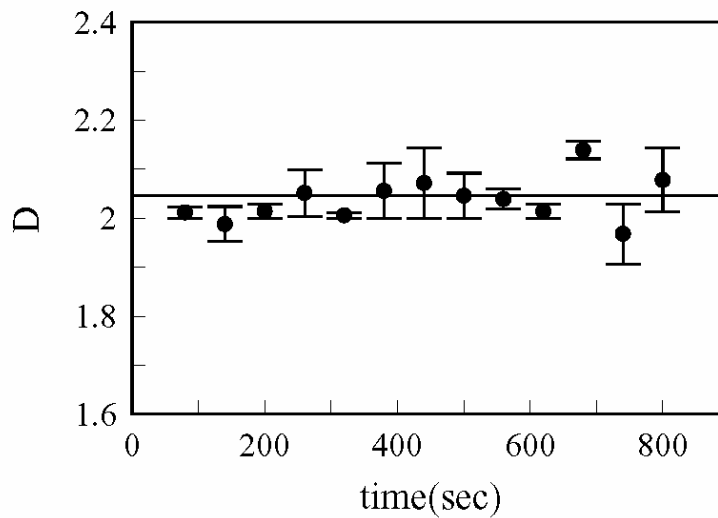


Fig.5 Plot of the fractal dimension D vs electrodeposition time t determined by the R/S analysis. The horizontal line indicates an average value of D , 2.04 ± 0.02 .

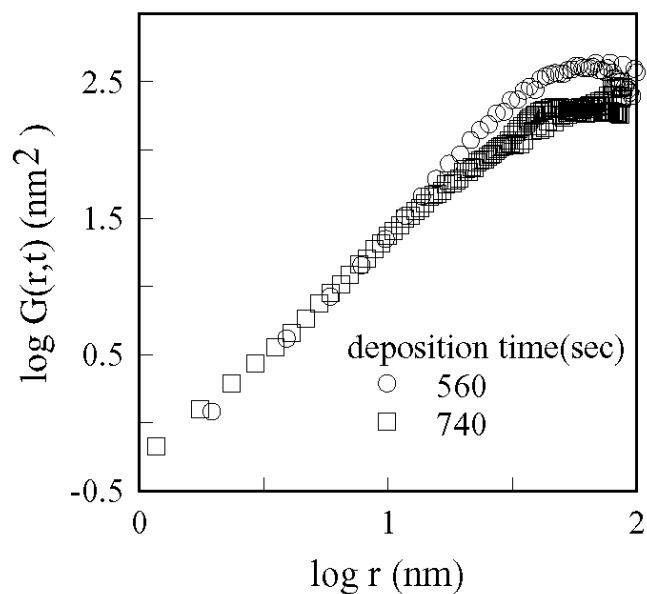


Fig.6 Log-log plot of the height-difference correlation functions $G(r,t)$ vs r , calculated from the AFM images of the electrodeposited nickel films.

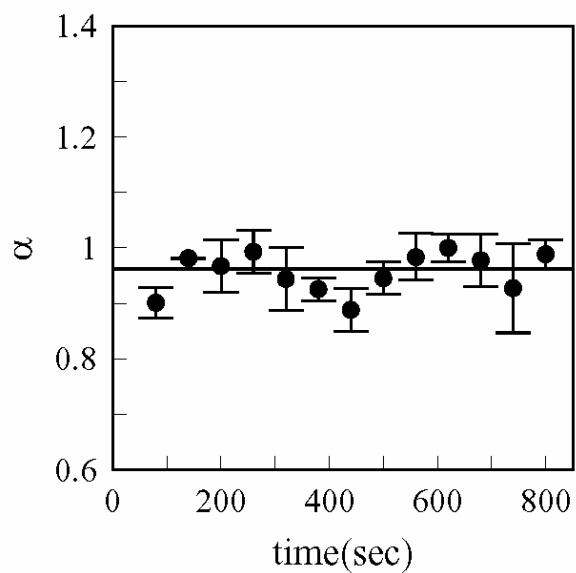


Fig.7 Plot of the roughness exponent α vs electrodeposition time t determined from the slopes in Fig.6. The horizontal line indicates an average value of α , 0.96 ± 0.04 .

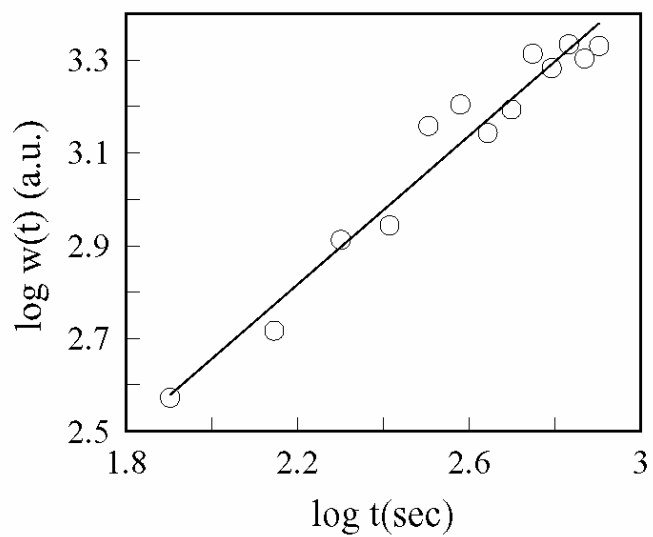


Fig.8 Log-log plot of the interface width $w(t)$ vs electrodeposition time t , calculated from Eq.(7). The solid line indicates a straight line with the slope β of 0.80 ± 0.07 best fitted to the data.